The carboxy-terminal insert in the Q-loop is needed for functionality of Escherichia coli cytochrome bd-I

Ghasemi Goojani, Hojjat Allah; Konings, Julia; Hakvoort, Henk; Hong, Sangjin; Gennis, Robert B.; Sakamoto, Junshi; Lill, Holger; Bald, Dirk

published in
Biochimica et Biophysica Acta - Bioenergetics
2020

DOI (link to publisher)
10.1016/j.bbabio.2020.148175

document version
Publisher's PDF, also known as Version of record

BBA - Bioenergetics 1861 (2020) 148175

Contents lists available at ScienceDirect

BBA - Bioenergetics

journal homepage: www.elsevier.com/locate/bbabio

The carboxy-terminal insert in the Q-loop is needed for functionality of *Escherichia coli* cytochrome *bd*-I

Hojjat Ghasemi Goojani[a], Julia Konings[a], Henk Hakvoort[a], Sangjin Hong[b], Robert B. Gennis[b], Junshi Sakamoto[c], Holger Lill[a], Dirk Bald[a,*]

[a] Department of Molecular Cell Biology, Amsterdam Institute for Molecules, Medicines and Systems, Faculty of Sciences, Vrije Universiteit Amsterdam, De Boelelaan 1108, 1081 HZ Amsterdam, the Netherlands
[b] Department of Biochemistry, University of Illinois, 600 S. Mathews Avenue, Urbana, IL 61801, United States
[c] Department of Bioscience and Bioinformatics, Kyushu Institute of Technology, Kawazu 680-4, Iizuka, Fukuoka-ken 820-8502, Japan

ARTICLE INFO

Keywords:
Cytochrome *bd*
Terminal oxidase
Q-loop
Mutagenesis
Biochemistry

ABSTRACT

Cytochrome *bd*, a component of the prokaryotic respiratory chain, is important under physiological stress and during pathogenicity. Electrons from quinol substrates are passed on via heme groups in the CydA subunit and used to reduce molecular oxygen. Close to the quinol binding site, CydA displays a periplasmic hydrophilic loop called Q-loop that is essential for quinol oxidation. In the carboxy-terminal part of this loop, CydA from *Escherichia coli* and other proteobacteria harbors an insert of ~60 residues with unknown function. In the current work, we demonstrate that growth of the multiple-deletion strain *E. coli* MB43Δ*cydA* (Δ*cydA*Δ*cydB*Δ*appB*Δ*cyoB*Δ*nuoB*) can be enhanced by transformation with *E. coli* cytochrome *bd*-I and we utilize this system for assessment of Q-loop mutants. Deletion of the cytochrome *bd*-I Q-loop insert abolished MB43Δ*cydA* growth recovery. Swapping the cytochrome *bd*-I Q-loop for the Q-loop from *Geobacillus thermodenitrificans* or *Mycobacterium tuberculosis* CydA, which lack the insert, did not enhance the growth of MB43Δ*cydA*, whereas swapping for the Q-loop from *E. coli* cytochrome *bd*-II recovered growth. Alanine scanning experiments identified the cytochrome *bd*-I Q-loop insert regions Ile^{318}-Met^{322}, Gln^{338}-Asp^{342}, Tyr^{353}-Leu^{357}, and Thr^{368}-Ile^{372} as important for enzyme functionality. Those mutants that completely failed to recover growth of MB43Δ*cydA* also lacked oxygen consumption activity and heme absorption peaks. Moreover, we were not able to isolate cytochrome *bd*-I from these inactive mutants. The results indicate that the cytochrome *bd* Q-loop exhibits low plasticity and that the Q-loop insert in *E. coli* is needed for complete, stable, assembly of cytochrome *bd*-I.

1. Introduction

Cytochrome *bd* is a terminal oxidase found in the respiratory chain of prokaryotes. The enzyme is located in the bacterial cytoplasmic membrane and oxidizes quinol-type substrates such as ubiquinol or menaquinol, coupled to reduction of molecular oxygen to water [1]. In particular, cytochrome *bd* is important under conditions of stress, such as O_2-limitation [2,3] and in the presence of nitric oxide [4–7]. In a variety of pathogenic bacteria, cytochrome *bd* is required during infection in the mammalian host, e.g. in *Staphylococcus aureus* [8] and in uropathogenic *Escherichia coli* strains [7,9]. In *Mycobacterium tuberculosis* and related mycobacterial strains cytochrome *bd* has been shown to participate in the defense against antibiotics [10–16].

Cytochrome *bd* has been purified from a variety of Gram-positive and Gram-negative bacterial strains including *E. coli* [17,18], *Azotobacter vinelandii* [20], *Geobacillus thermodenitrificans* (strain K1041, formerly called *Bacillus stearothermophilus*) [21,22], and *Corynebacterium glutamicum* [23]. From *E. coli*, two *bd*-type quinol oxidases have been isolated, referred to as cytochrome *bd*-I and cytochrome *bd*-II [24,25]. Across species, cytochrome *bd* consists of the two major subunits CydA and CydB that carry three non-covalently bound heme groups, namely hemes b_{558}, b_{595} and *d*. Next to these major subunits cytochrome *bd*-I from *E. coli* comprises two additional, smaller subunits: one termed CydX [26,27] and a second one termed either CydH [28] or CydY [29]. A different small subunit, CydS, was found in the *G. thermodenitrificans* enzyme [22].

The crystal structure of cytochrome *bd* from *G. thermodenitrificans* revealed that all three heme groups, along which electrons derived from the quinol are transferred to molecular oxygen, are bound to the CydA subunit [22]. In proximity of heme b_{558}, which accepts the electrons

* Corresponding author.
E-mail address: d.bald@vu.nl (D. Bald).

https://doi.org/10.1016/j.bbabio.2020.148175
Received 21 August 2019; Received in revised form 24 January 2020; Accepted 10 February 2020
Available online 12 February 2020
0005-2728/

from the quinol substrate [30], a large hydrophilic loop is located between trans-membrane helices 6 and 7 of CydA, on the periplasmic side of the membrane [22,31] (purple loop in Fig. 1A). This loop, referred to as Q-loop, has been identified as instrumental for quinol binding [32,33]. The Q-loop of cytochrome *bd* from *G. thermodenitrificans* consists of ~80 amino acid residues [22], consistent with the length of this loop in most bacterial species, as inferred from sequence data [1,34]. However in some bacterial species, e.g. *E. coli*, *A. vinelandii* and other proteobacteria, cytochrome *bd* carries an insert of ~60 residues in the carboxy-terminal part of the Q-loop (Fig. 1B, insert residues depicted in blue). Regions and individual residues in the Q-loop that are important for cytochrome *bd* activity have previously been reported based on proteolysis by trypsin or chymotrypsin [32,33], binding of monoclonal antibodies [35,36], site-directed mutagenesis [37], and quinol-labeling studies [38]. Interestingly, the residues identified by these studies all mapped to the N-terminal part of the Q-loop, none of them is located in the C-terminal insert. Cytochrome *bd* from *G. thermodenitrificans,* whose crystal structure was known when we initiated and conducted our study, lacks the C-terminal Q-loop insert and the role of the C-terminal Q-loop insert is obscure.

In the current report we employ domain swap approaches, alanine scanning and site-directed mutagenesis to investigate the function of the C-terminal Q-loop insert of *E. coli* cytochrome *bd*-I.

2. Material & methods

2.1. Construction of expression vectors

2.1.1. Replacement of MB43 cydA by the superfolder GFP gene

The *cydA* gene was replaced by the superfolder-GFP gene using a CRISPR/Cas9 two-plasmid system [39]. Primers and templates are listed in Supplementary Table 1. On a pTarget vector an sgRNA targeting *cydA* was created by replacing the N20 region with a 20 bp fragment of the *cydA* gene (using N20 primer pairs). After performing this PCR, the product was purified and self-ligated using the Gibson assembly kit (NEB). In a next step, a complementary region ("UpCydA_sfGFP_CydX") was introduced into this pTargetN20*cydA* vector. This linear, overlapping-end PCR product was produced in consecutive PCR steps: first, a linear PCR product was generated using genomic DNA from *E. coli* MB43 as template using primer pairs (upcydAdowncydX). This linear PCR product was purified and used as template to generate the 300 bp fragment upstream of cydA ("UpCydA") and a 300 bp fragment downstream of and including cydX ("downCydX"), both with overhang complementary to sfGFP, using primer pairs ("Up-cydAptarget", "Down-cydXptarget"), respectively. Second, on pet16B_sfGFP a linear sfGFP fragment with overhang complementary to CydA and CydX was generated (primer pairs sfGFP). Third, on pTargetN20CydA a linear

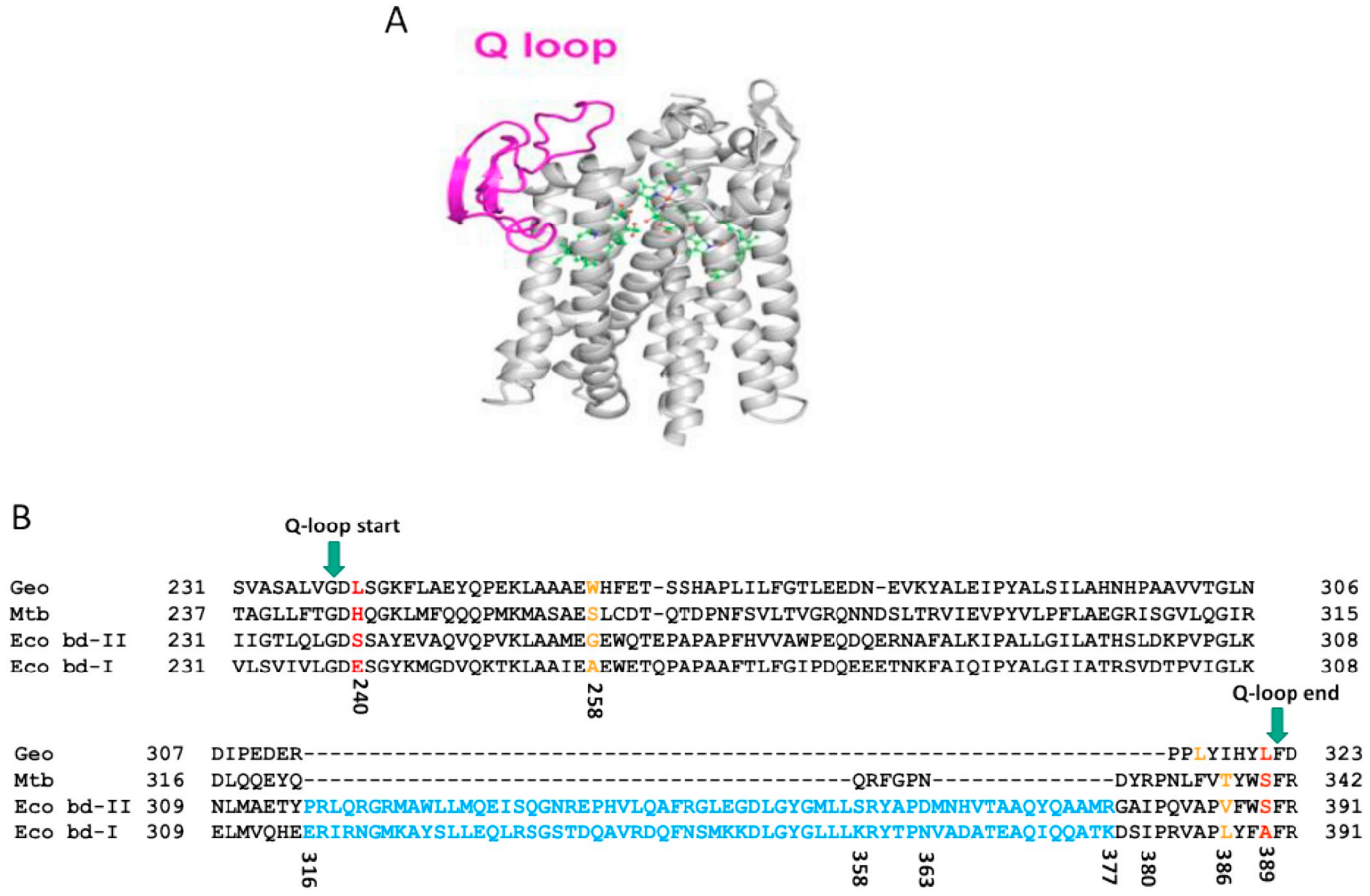

Fig. 1. The main cytochrome *bd* subunit CydA with the Q-loop. A: Structure of CydA from *G. thermodenitrificans*. The Q-loop is depicted in purple and the three heme groups are shown in ball-and-stick mode. B: Sequence alignment of the Q-loop amino acid residues from various species. Geo: *G. thermodenitrificans,* Mtb*: M. tuberculosis,* Eco: *E. coli*. The Q-loop insert found in *E. coli* and other proteobacteria is highlighted in blue. Positions used in this study for swapping the Q-loop between species are indicated either in red (240–389) or brown (258–386).

PCR fragment was generated with overhang on UpCydA and CydX (Primer pairs "Ptarget"). All fragments where assembled using the Gibson assembly kit (NEB). The plasmid was cloned and purified and transformed into MB43. Transformation and plasmid curing were performed as described [39]. The genomic insert sequence was confirmed using a specific insert primer and a primer outside the complementary region (Supplementary Fig. 1).

2.1.2. Q-loop mutants

For an overview of the constructed mutants please refer to Supplementary Fig. 1. Preparation of Q-loop mutants was based on a pET17b vector containing *cydABX* with the sequence encoding strep-tag II and a linker fused downstream of *cydX* [27]. The primers used to make new constructs are listed in Supplementary Table 1. Plasmids encoding mutants with shortened or lacking Q-loop insert were constructed by amplifying pET17b*cydABX* using primer pairs "*Ecoli* insert Mtb" and "*Ecoli* insert Geo" (Supplementary Table 1), respectively and subsequently fusing the resulting fragment by Gibson assembly cloning kit (NEB).

For constructing the plasmid encoding the mutant carrying a Ser/Gly linker instead of the *E. coli* Q-loop insert we started out with the existing linker [27] separating the *cydX* gene from the strep-tag. We added two additional, shortened copies of this linker using the primers and restriction sites listed in Supplementary Table 1 and finally transferred the complete 186 bp (coding for 62 residues) fragment into pET17B*cydABX* using *Bam*HI and *Eco*RI restriction sites. Gibson assembly was used for constructs with Q-loop swap mutants. pET17b*cydABX* and the sequence encoding the Q-loop from *G. thermodenitrificans* or *M. tuberculosis* or from *E. coli* cytochrome *bd*-II were amplified and fused. To re-insert the sequence for the *E. coli* Q-loop insert into the mutants with swapped Q-loop (Geo $^{(240–389)}$ and Mtb $^{(240–389)}$) the Geo $^{(240–389)}$ and Mtb $^{(240–389)}$ constructs and the sequence encoding *E. coli* Q-loop insert (or the *bd*-II insert) were amplified and fused. Alanine scanning mutants were made using primer pairs containing 5 alanine-encoding codons at the 5′ end (Supplementary Table 1). After amplification of pET17b*cydABX* Gibson assembly was used to fuse fragment ends.

For all constructed vectors, the correct sequence was confirmed by DNA sequencing.

2.2. Bacterial growth assays

Pre-cultures of *E. coli* MB43, MB43Δ*cydA* or MB43Δ*cydA* transformed with plasmids expressing WT cytochrome *bd*-I or Q-loop mutants were incubated in 5 mL Luria Bertani (LB) medium with 100 μg/mL ampicillin overnight at 37 °C while shaking at 200 rpm. From each pre-culture, a small volume was diluted to OD_{600} = 0.01 with 1.5 mL LB medium containing 100 μg/mL ampicillin. Each diluted sample was distributed over 6 wells of a 96-well microtiter plate. The plates were then incubated at 37 °C for 24 h (shaking at 200 rpm) in a SpectraMax Plus 384 Microplate reader, the OD_{600} was measured every 5 min.

2.3. Membrane isolation and protein purification

Isolation of cytoplasmic membrane fractions and purification of cytochrome *bd*-I was done based on Hoeser et al. [27]. MB43Δ*cydA* transformed with plasmids expressing WT cytochrome *bd*-I or Q-loop mutants were cultured in 800 mL LB medium (2-liter baffled flasks) overnight from a starting OD_{600} = 0.01 until late exponential phase. Cells were harvested, washed with phosphate buffer saline and then frozen and stored at −20 °C. Batches of frozen cells (5 g) were suspended in a 5-fold volume of 50 mM 3-(N-morpholino)propanesulfonic acid (MOPS), 100 mM NaCl, one tablet Complete (protease inhibitor), pH 7.0 ("MOPS buffer"). Suspended cells were disrupted by passing through a Stansted homogenizer at 1.2 kbar. Cell debris was removed by 20 min centrifugation at 9500 ×*g* and 4 °C. The membrane fractions were then pelleted by ultracentrifugation for 75 min at 250,000 ×*g* and 4 °C. Batches of frozen membranes were resuspended in MOPS-buffer containing 0.025% n-dodecyl-β-D-maltoside (DDM) using a homogenizer, and used for either protein purification or membrane oxygen consumption activity assays.

For purification of cytochrome *bd*-I, the suspended membranes were diluted to a final protein concentration of 10 mg/mL (determined by BCA assay). To solubilize the membrane protein, 1% DDM (final conc.) was added, and incubated at 4 °C for 1 h on a roller incubator. Insolubilized material was sedimented by ultracentrifugation at 250,000 ×*g* for 15 min at 4 °C. The supernatant was applied to a 1 mL strep-tactin gravity flow column (IBA Lifesciences). Unspecifically bound protein was removed by addition of 5 mL washing buffer (50 mM sodium phosphate, 300 mM NaCl, 1 tablet Complete protease inhibitor, 0.01% DDM, pH 8.0). Finally, the cytochrome *bd*-I was eluted by adding 250 μL elution buffer (washing buffer containing 2.5 mM desthiobiotin). All steps were executed at 4 °C.

2.4. Oxygen consumption activity

Oxygen consumption activity of isolated membrane fractions and of purified cytochrome *bd*-I was measured using a Clark-type electrode based on Lu et al. [40]. The membrane fractions (final conc. ~5 μg/mL) or the purified cytochrome *bd*-I (final conc. 1–2.5 nM, depending on type of mutant) were incubated in 600 μL MOPS buffer containing 0.025% DDM at 37 °C in the electrode chamber. The substrates ubiquinone-1 and dithiothreitol (DTT) were first pre-incubated separately for 3 min at 37 °C and then injected into the electrode chamber to start the reaction (final conc. 200 μM ubiquinone-1 and 10 mM DTT). The reaction rate was determined for the period between 90 s and 150 s after addition of the substrate mix. Rates were corrected for the signal change observed in the same interval for the substrate mix alone (without membranes or purified protein). Data were analyzed using one-way ANOVA.

2.5. Heme spectra analysis

The heme group content of cytoplasmic membranes isolated from *E. coli* MB43Δ*cydA* expressing WT cytochrome *bd*-I or Q-loop mutants was measured by the reduced minus oxidized UV-VIS spectrum. The isolated membrane fractions were diluted to a protein concentration of 2.6 mg/mL in 10 mM tris-(hydroxymethyl)aminoethane (TRIS)/HCl, pH 7.4, 16 mM sodium cholate [3]. Samples were oxidized with 100 μM potassium ferricyanide and the spectrum was recorded at room temperature (Varian Cary 50 UV–Vis Spectrophotometer). Subsequently, a few grains of solid sodium hydrosulfite were dissolved in the sample to measure the spectrum in the reduced state. The difference spectrum (reduced-oxidized) was calculated and normalized to protein concentration. The heme content for purified proteins was measured with the same method, but using 50 μg/mL of purified proteins dissolved in 50 mM MOPS, 300 mM NaCl and 0.01% DDM, pH 8.

2.6. SDS-PAGE

Protein purity was monitored by sodium dodecyl sulfate polyacrylamide gel electrophoresis using a 4–20% gradient gel as described [41]. Proteins were stained either with Coomassie Brilliant Blue or with silver.

3. Results

3.1. E. coli strain MB43ΔcydA as a platform for monitoring cytochrome bd-I function

To evaluate the functionality of cytochrome *bd*-I mutants we utilized *E. coli* strain MB43 [42]. This strain carries multiple mutations in

respiratory chain genes including *cydB* (cytochrome *bd*-I) *appB* (cytochrome *bd*-II) *cyoB* (cytochrome bo_3) and *nuoB* (type-I NADH dehydrogenase). As a consequence, growth of MB43 is strongly decreased as compared to wild-type *E. coli* [42]. We speculated that introduction of genes coding for functional cytochrome *bd*-I may enhance growth of MB43 and may allow for screening of mutants. However, MB43 still carries an intact genomic copy of the *cydA* gene that could preclude proper assessment of Q-loop mutations (located in CydA) expressed from a plasmid. So we first deleted the *cydA* gene of MB43 strain and replaced it by superfolder-GFP using a CRISPR/Cas9 two-plasmid system [39] (Supplementary Fig. 2). Similar to the MB43 parent strain, MB43Δ*cydA* showed strongly attenuated growth, with a maximal OD_{600} ~ 0.2 reached after 24 h of incubation in LB medium (Fig. 2A).

We then introduced the *cydABX* genes (pET17b*cydABX*, [27]), encoding wild-type cytochrome *bd*-I, into the newly generated MB43Δ*cydA* strain and monitored bacterial growth using a microplate reader. Expression of wild-type cytochrome *bd*-I considerably stimulated growth (maximum OD_{600} of ~0.5 after 10 h), whereas introduction of the empty vector control did not recover growth (Fig. 2A). These results show that the MB43Δ*cydA* strain can be used as a convenient system for assessment of cytochrome *bd*-I functionality.

3.2. Importance of the C-terminal Q-loop insert for cytochrome bd-I functionality

To assess the importance of the C-terminal Q-loop insert in *E. coli* cytochrome *bd*-I, we constructed mutants with shortened or deleted insert. In the first mutant we deleted the C-terminal Q-loop insert (Glu^{316}-Pro^{381}), based on sequence comparison to cytochrome *bd* from *G. thermodenitrificans* (see Fig. 1B). In a second mutant we shortened the C-terminal insert of *E. coli* cytochrome *bd*-I to the length of the insert present in the *M. tuberculosis* enzyme. To construct this second mutant we removed the region Glu^{316}-Lys^{377} from *E. coli* CydA, with the exception of the sequence Lys^{358}-Asn^{363}, which is homologous to the six-residue "island" Gln^{323}-Asn^{328} in CydA from *M. tuberculosis* (Fig. 1B). Transformation of both mutant plasmids did not enhance the growth of the MB43Δ*cydA* strain (Fig. 2B). Upon deletion or pronounced shortening of the C-terminal insert, cytochrome *bd*-I apparently is not sufficiently functional to support growth. This lack of functionality may be caused by a need for an insert of a certain length, independent of the specific amino acid composition. Therefore, we replaced the *E. coli* Q-loop insert (Glu^{316}-Lys^{377}) by a Gly-Ser linker of the same length. However, transforming the mutant plasmid carrying this Gly-Ser insert in CydA did not recover the growth of MB43Δ*cydA* (Fig. 2B). These results suggest that the C-terminal Q-loop insert, although not conserved across species, is required for cytochrome *bd*-I functionality.

3.3. Impact of Q-loop domain swap on functionality of cytochrome bd-I

The lack of functionality observed for the mutants described above may be caused by specific interactions between N-terminal and C-terminal parts of the Q-loop. To address this issue, we exchanged the whole Q-loop of *E. coli* cytochrome *bd*-I by the Q-loop from the *G. thermodenitrificans* and *M. tuberculosis* enzymes. We replaced *E. coli* CydA residues Glu^{240}-Ala^{389} by Leu^{240}-Leu^{321} from *G. denitrificans* or His^{246}-Ser^{340} from *M. tuberculosis* CydA (see Fig. 1B). These two mutants did not show functional cytochrome *bd*-I in the MB43Δ*cydA* growth assay (Fig. 2C).

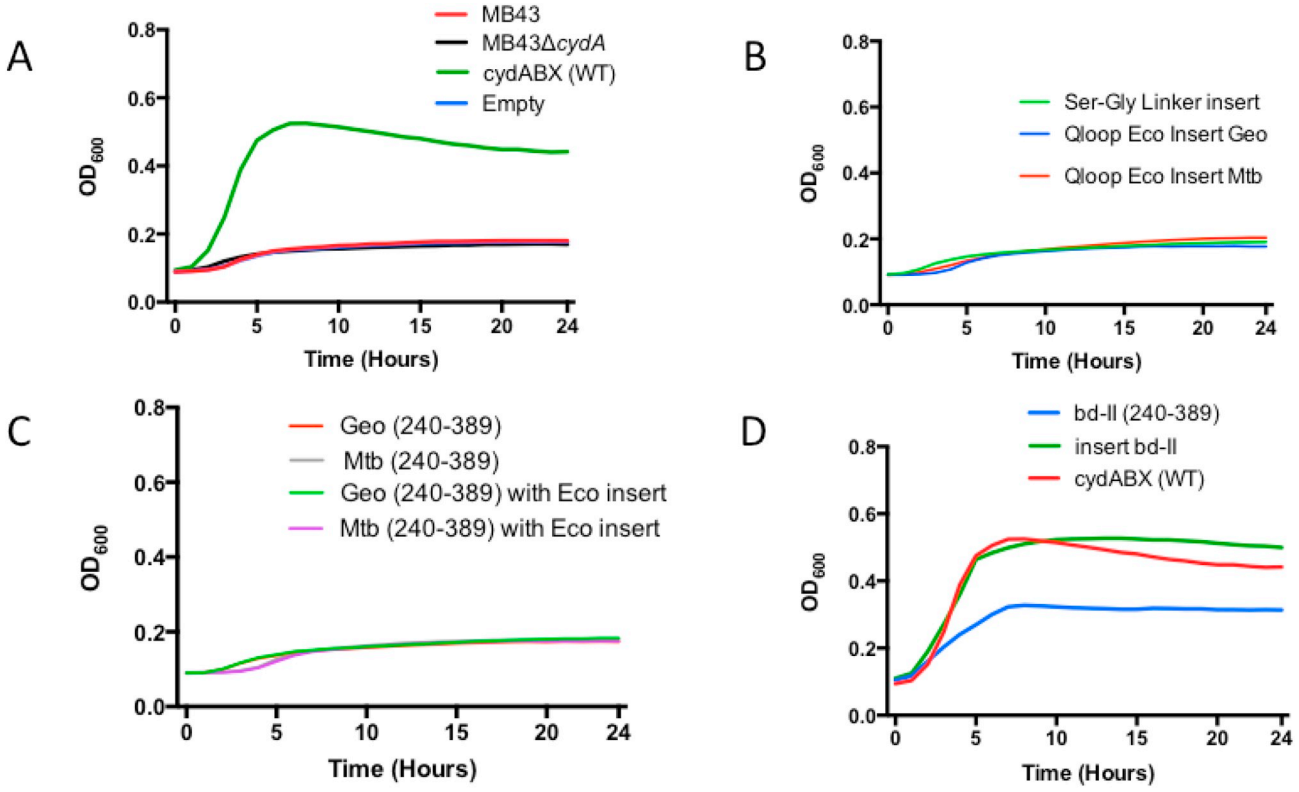

Fig. 2. Growth of *E. coli* MB43Δ*cydA* transformed with cytochrome *bd*-I mutants. A: Growth curve of MB43 parent strain, MB43Δ*cydA* and MB43Δ*cydA* transformed with the cytochrome *bd*-I expression vector pET17b*cydABX*. B–D: Growth curve of MB43Δ*cydA* transformed with *cydA* mutants. B: Q-loop Eco insert Geo and Q-loop Eco insert Mtb represent mutants with the Q-loop insert shortened according to *G. thermodenitrificans* and *M. tuberculosis,* respectively. Ser-Gly linker: mutant with the Q-loop insert replaced by a 62-residue Gly/Ser linker. C: CydA mutants with *E. coli* Q-loop (position 240–389) swapped for either the *G. thermodenitrificans* or *M. tuberculosis* Q-loop, with or without the Q-loop insert from *E. coli* CydA. D: bd-II (240–389): CydA mutant with the Q-loop replaced by the Q-loop from *E. coli* cytochrome *bd*-II. "Insert bd-II": CydA mutant with Q-loop insert replaced by the Q-loop insert from *E. coli* cytochrome *bd*-II. Growth was followed with a microplate reader and samples were in 200 μL LB medium containing 100 μg/ml ampicillin. For more details, please refer to Material & methods.

In a second approach we replaced *E. coli* residues Ala^{258}-Leu^{386} by the corresponding residues Trp^{258}-Leu^{316} from *G. thermodenitrificans* or Ser^{264}-Thr^{337} from *M. tuberculosis* CydA (Fig. 1B). This approach leaves residues Lys^{252} and Glu^{257} (*E. coli* numbering), two residues that are essential for enzymatic activity [37], unchanged. However, these mutants did not recover the growth of MB43Δ*cydA,* either (data not shown).

Similarly, "re-insertion" of the C-terminal *E. coli* CydA insert into the mutants carrying the *Geobacillus* Q-loop (Glu^{316}-Ile^{380} inserted between Arg^{313} and Pro^{314}) or the *Mycobacterium* Q-loop (Lys^{323}-Asn^{328} replaced by Glu^{316}-Lys^{377}) did not recover growth of MB43Δ*cydA* (Fig. 2C). These results indicate a low plasticity of the Q-loop in general and of the C-terminal insert in particular.

Subsequently, we replaced the Q-loop of *E. coli* cytochrome *bd*-I by the Q-loop from *E. coli* cytochrome *bd*-II. The CydA subunit of cytochrome *bd*-I and the homologous subunit from cytochrome *bd*-II, referred to as AppC, share 69% sequence identity and AppC features a C-terminal Q-loop insert of the same length as and ~60% sequence similarity to CydA (Fig. 1B). This mutation (CydA Glu^{240}-Ala^{389} replaced by AppC Ser^{240}-Ser^{389}) partially recovered the growth of MB43Δ*cydA*, indicating a functional cytochrome *bd*-I (Fig. 2D). When only the C-terminal insert was swapped between *bd*-I and *bd*-II (CydA Glu^{316}-Lys^{377} replaced by AppC Pro^{316}-Arg^{377}), bacterial growth virtually fully recovered (Fig. 2D). Apparently, the function of the C-terminal insert in *E. coli* CydA can be taken over by the insert from a homologous enzyme with sufficient sequence similarity.

3.4. Alanine scanning of the C-terminal Q-loop insert

To pinpoint which regions in the Q-loop insert are crucial for cytochrome *bd*-I functionality we employed an alanine-scanning approach. We constructed 13 mutants, in each of which five consecutive residues were replaced by alanine (Fig. 3A). Among these 13 mutants, 9 recovered growth of MB43Δ*cydA* similar to wild-type cytochrome *bd*-I, whereas the mutants with residues Ile^{318}-Met^{322}, Gln^{338}-Asp^{342}, Tyr^{353}-Leu^{357}, and Thr^{368}-Ile^{372} replaced by alanine showed growth as observed for the empty vector control (Fig. 3B, C). This result suggests that the low degree of plasticity observed for the C-terminal insert is conferred by these four regions.

3.5. Activity of cytochrome bd-I Q-loop mutants in isolated membranes

We assessed cytoplasmic membranes isolated from the cytochrome *bd*-I mutant strains for enzymatic activity. Membranes from the wild-type strain showed a specific oxygen consumption activity of 2.5 μmol O_2/mg/min with ubiquinol-1/dithiothreitol as substrate (Fig. 4A). In contrast, membranes isolated from the mutants with shortened C-terminal insert or mutants with the whole Q-loop replaced by the *Mycobacterium* or *Geobacillus* Q-loop did not show detectable oxygen consumption activity (Fig. 4A). This result reveals that the lack of growth recovery observed for these mutants is indeed caused by absence of enzymatic activity. The mutants carrying either the whole Q-loop or the C-terminal insert derived from cytochrome *bd*-II both showed substantial oxygen consumption activity (Fig. 4A). For the

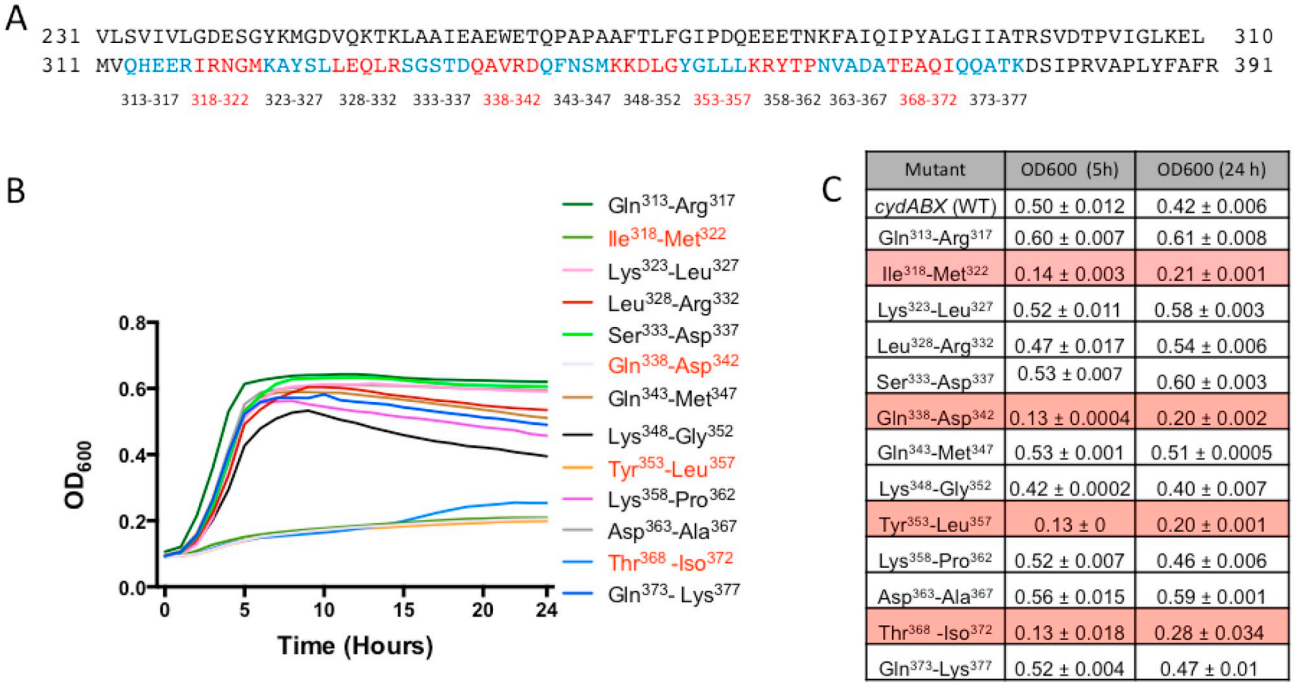

Mutant	OD600 (5h)	OD600 (24 h)
cydABX (WT)	0.50 ± 0.012	0.42 ± 0.006
Gln^{313}-Arg^{317}	0.60 ± 0.007	0.61 ± 0.008
Ile^{318}-Met^{322}	0.14 ± 0.003	0.21 ± 0.001
Lys^{323}-Leu^{327}	0.52 ± 0.011	0.58 ± 0.003
Leu^{328}-Arg^{332}	0.47 ± 0.017	0.54 ± 0.006
Ser^{333}-Asp^{337}	0.53 ± 0.007	0.60 ± 0.003
Gln^{338}-Asp^{342}	0.13 ± 0.0004	0.20 ± 0.002
Gln^{343}-Met^{347}	0.53 ± 0.001	0.51 ± 0.0005
Lys^{348}-Gly^{352}	0.42 ± 0.0002	0.40 ± 0.007
Tyr^{353}-Leu^{357}	0.13 ± 0	0.20 ± 0.001
Lys^{358}-Pro^{362}	0.52 ± 0.007	0.46 ± 0.006
Asp^{363}-Ala^{367}	0.56 ± 0.015	0.59 ± 0.001
Thr^{368} -Iso^{372}	0.13 ± 0.018	0.28 ± 0.034
Gln^{373}-Lys^{377}	0.52 ± 0.004	0.47 ± 0.01

Fig. 3. Alanine scanning mutagenesis of the Q-loop insert. A: Q-loop residues from *E. coli* CydA. The insert (Gln^{313}-Lys^{377}) is depicted in blue/red. For each alanine scanning mutant, five consecutive residues were replaced by alanine. B: Growth curves of MB43Δ*cydA* transformed with the alanine mutants incubated on a microplate reader. C: Average OD_{600} and standard error of the mean (SEM) after 5 h and 24 h of growth shown for two biological replicates (each including six wells per mutant). Mutants that completely failed to recover growth are marked with reddish shading.

mutant carrying the whole Q-loop from cytochrome *bd*-II the enzymatic activity (~60% of wild-type activity) reflected the degree of growth recovery observed in the MB43Δ*cydA* system (~50% compared to wild-type), whereas for the mutant carrying only the C-terminal Q-loop insert from cytochrome *bd*-II the oxygen consumption activity (~20% of wild-type) was relatively low (Fig. 4A), although growth recovery of MB43Δ*cydA* was virtually complete (Fig. 2C).

Among the alanine-scanning Q-loop mutants that recovered growth of MB43Δ*cydA,* several mutants (Lys^{323}-Leu^{327}, Ser^{333}-Asp^{337}, Gln^{343}-Met^{347}, Lys^{358}-Pro^{362}, Asp^{363}-Ala^{367}) displayed oxygen consumption activity similar to the wild-type enzyme, whereas others (Gln^{313}-Arg^{317}, Leu^{328}-Arg^{332}, Lys^{348}-Gly^{352}, Gln^{373}-Lys^{377}) were significantly less active (Fig. 4B). This might be explained by a certain degree of elasticity linking respiratory chain activity to bacterial growth, but also indicates a limitation of the employed MB43 Δ*cydA* growth assay. Importantly, we did not detect any oxygen consumption activity for Ile^{318}-Met^{322}- > Ala, Gln^{338}-Asp^{342}- > Ala, Tyr^{353}-Leu^{357}- > Ala and Thr^{368}-Ile^{372}- > Ala, those alanine-scanning mutants that did not recover growth of MB43Δ*cydA* (Fig. 4B). Apparently, relatively minor changes introduced into the C-terminal Q-loop insert can already be sufficient to abolish the enzymatic activity of cytochrome *bd*-I.

3.6. Heme-content of cytochrome bd-I Q-loop mutants

Lack of cytochrome *bd* activity can be caused by insufficient enzyme assembly/stability or alternatively by a properly assembled but inactive enzyme. To shed light on cytochrome *bd*-I assembly we investigated the effect of Q-loop mutations on the heme group content in the isolated cytoplasmic membranes. Proper binding of heme b_{558}, heme b_{595}, and heme *d* is required for complete assembly of the enzyme. Reduced-minus-oxidized difference absorption spectra recorded with isolated cytoplasmic membranes of MB43Δ*cydA* transformed with wild-type cytochrome *bd*-I showed clear peaks for heme b_{558} and heme *d* (630 nm), whereas the heme b_{595} peak was less resolved (Fig. 5A). These peaks were absent in the control sample transformed with the empty vector (Fig. 5A). Mutants carrying the whole Q-loop or the Q-loop insert derived from cytochrome *bd*-II showed heme b_{558} and heme *d* peaks, although less pronounced as compared to the wild-type enzyme (Fig. 5B). A similar pattern in the difference spectrum was observed for those alanine scanning mutants that yielded functional cytochrome *bd*-I (Fig. 5C). In contrast, Q-loop mutants that did not recover growth of MB43Δ*cydA* and were inactive in oxygen consumption, did not display heme b_{558} and heme *d* peaks (Fig. 5D,E). This result suggests that for these Q-loop mutants the assembly of cytochrome *bd*-I is incomplete.

3.7. Assembly/stability of the CydABX complex in cytochrome bd-I Q-loop mutants

Undetectable heme content in the inactive Q-loop mutants can be caused by local disturbance of the protein structure that prevents stable heme binding, but leaves the CydABX apo-complex intact. Alternatively, the assembly/stability of whole CydABX complex may be impaired. To distinguish between these two alternatives, we attempted to purify the CydABX complex from mutants that did not show any detectable oxygen consumption activity or heme absorption. We extracted membrane fractions from these mutants, passed the extract through a strep-tactin affinity column as reported earlier for purification of cytochrome *bd*-I [27], and assessed the eluate by SDS-gel electrophoresis. For purified wild-type cytochrome *bd*-I the major subunits were clearly detectable (Fig. 6). In contrast, only background bands resembling those observed in the empty vector control were found for

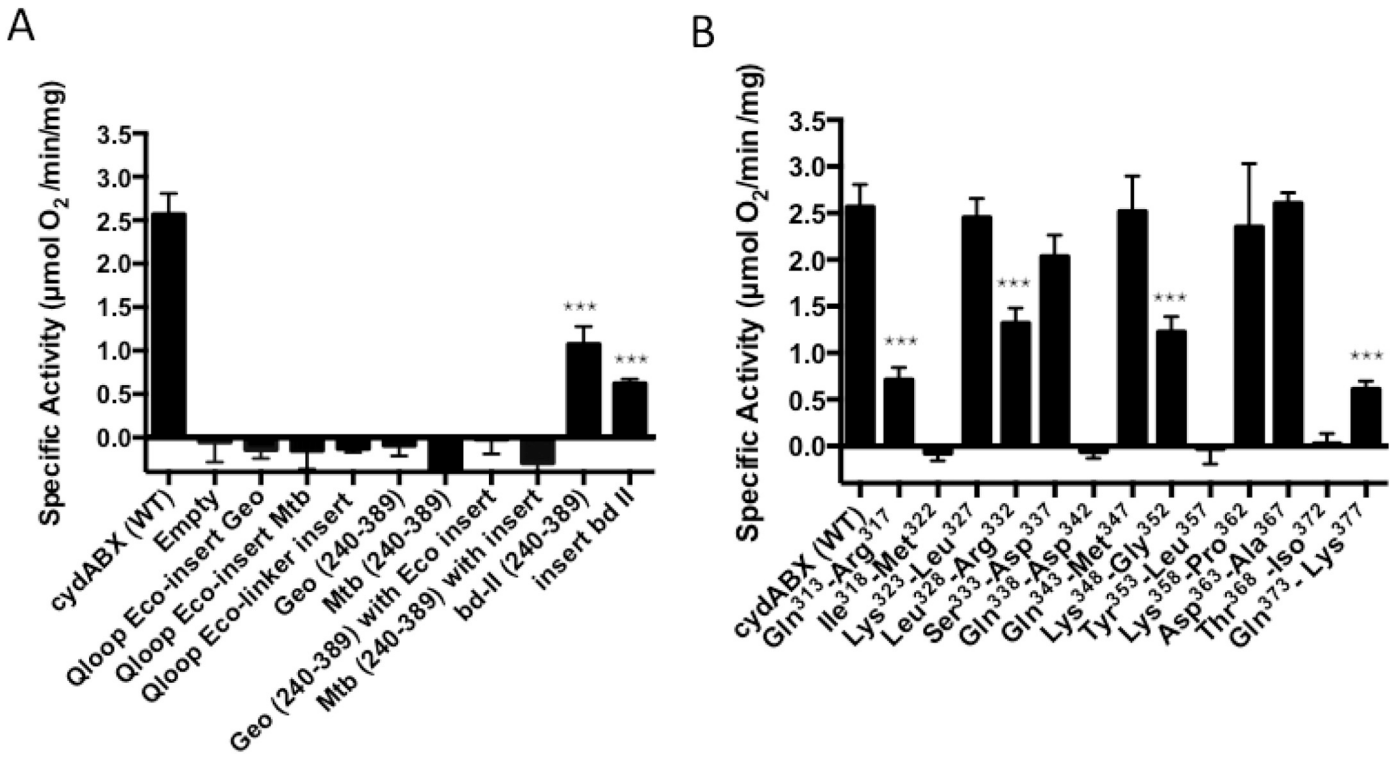

Fig. 4. Oxygen consumption activity of isolated cytoplasmic membrane fractions. Oxygen consumption was measured by a Clark-type electrode using ubiqunone-1 and DTT as substrate. A: Activity of mutants with shortened or swapped Q-loop, B: Activity of alanine scanning mutants. Presented values are averages from two biological replicates (comprising in total six technical replicates) and error bars represent SEM (★★★: $P < .001$, ★★: $P < .01$). For more details, please refer to Material & methods.

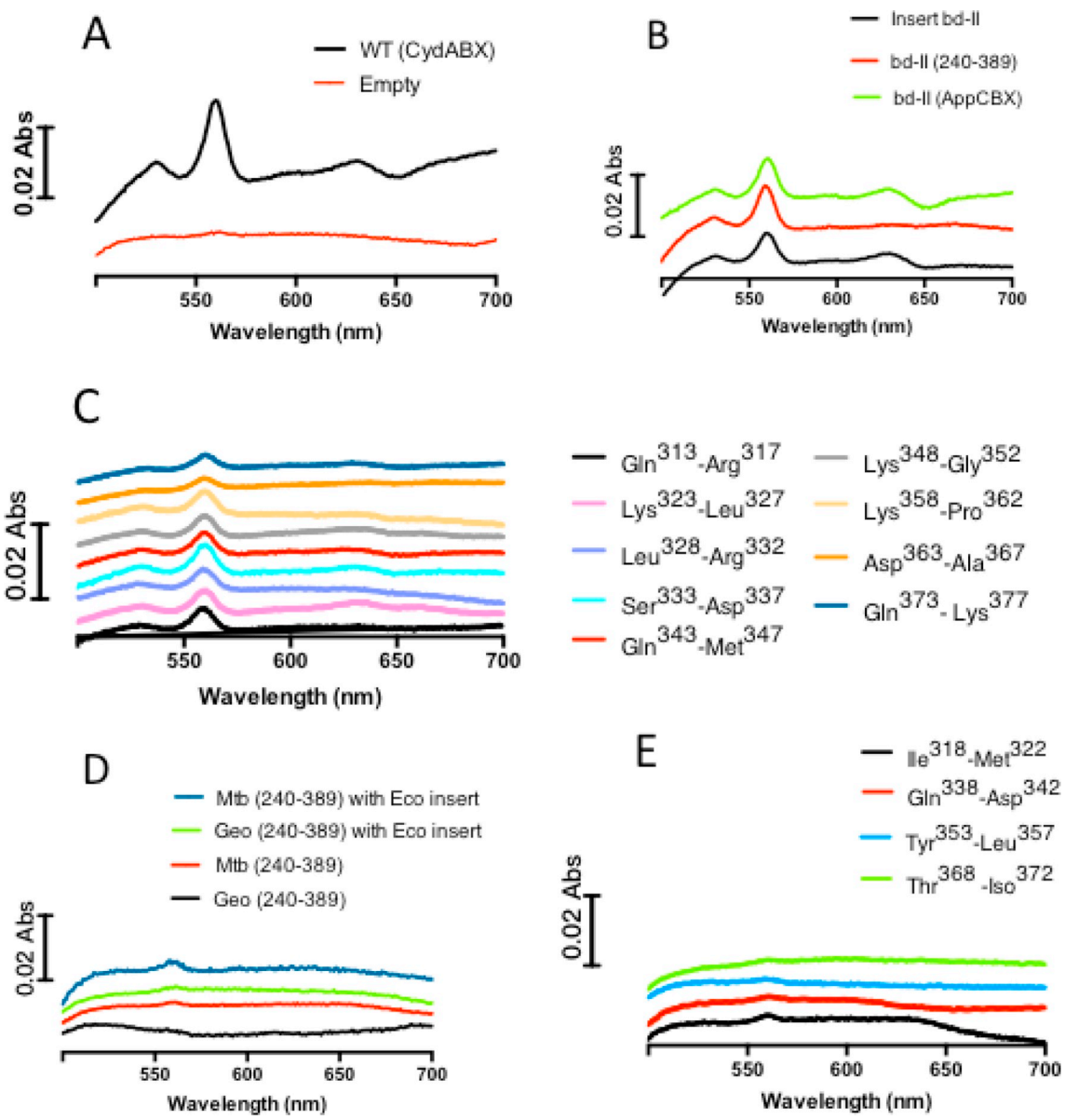

Fig. 5. Heme-content of cytochrome *bd*-I Q-loop mutants. Reduced-minus-oxidized absorption spectra were recorded using membrane fractions freshly isolated from: A, MB43Δ*cydA* transformed with the cytochrome *bd*-I expression vector pET17b*cydABX* or with empty vector control, B, domain swap mutants with bd-II Q-loop, C, alanine mutants with detectable oxygen consumption activity, D, domain swap mutants that did not show detectable oxygen consumption activity, E, alanine mutants that did not show detectable oxygen consumption activity. For each mutant, two biological replicates (in total at least six technical replicates) were investigated, representative results are shown. For more details, please refer to Material & methods.

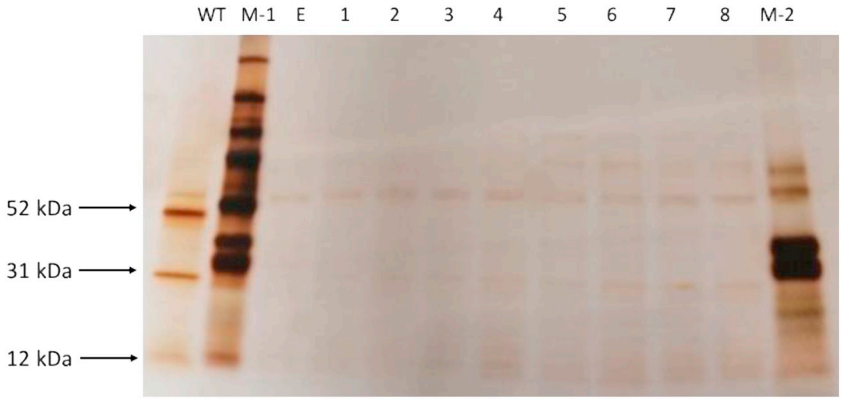

Fig. 6. SDS-gel electrophoresis of wild-type and mutant cytochrome *bd*-I purified by streptactin chromatography. Lane WT: wild-type CydABX, Lane M-1: full range marker, Lane E: empty vector, Lane 1: Insert-linker, Lane 2: Q-loop Ecoli-insert Geo, Lane 3: Q-loop Ecoli-insert Mtb, Lane 4: Q-loop Mtb (240–389), Lane 5: Q-loop Geo (240–389), Lane 6: Ile^{318}-Met^{322}, Lane 7: Gln^{338}-Asp^{342}, Lane 8: Thr^{368} -Ile^{372}, Lane M-2: low range marker. For each lane, 20 ng of purified protein was used.

the mutant strains (Fig. 6). As in the expression system we employ here the strep-tag is fused to CydX [27], these results reveal that the assembly of the CydABX complex is impaired.

3.8. Purification of Q-loop mutants with intermediate membrane activity

Mutants that displayed intermediate oxygen consumption activity at membrane level, (insert *bd*-II, Q-loop *bd*-II (240–389) and alanine mutants Gln^{313}-Arg^{317}, Leu^{328}-Arg^{332}, Lys^{348}-Gly^{352}, Gln^{373}-Lys^{377}), may either have less cytochrome *bd* present in the membrane or the cytochrome *bd* may have lower specific activity and/or heme content. We purified cytochrome *bd*-I from those mutant strains as described in the previous chapter. For these mutants, the yield of protein purified with a streptactin-affinity column was slightly lower as compared to the wild-type enzyme (73–93%) (Fig. 7A). SDS-gel electrophoresis did not reveal significant differences in purity between the purified Q-loop mutants (Fig. 7B). However, the specific enzymatic activity for all tested mutants was considerably lower as compared to the wild-type enzyme, with maximum activity measured for the Leu^{328}-Arg^{332}- > Ala mutant (50% relative to WT) and lowest activity found for the Lys^{348}-Gly^{352}- > Ala mutant (15% relative to WT) (Fig. 7C). Consistent with the lower enzymatic activity, the heme content in the mutants was decreased as compared to wild-type cytochrome *bd*-I (Fig. 7D).

4. Discussion

Previously, *E. coli* strains carrying multiple deletions in respiratory chain genes have been constructed to study the terminal oxidases [42]. Here, we showed that the multi-deletion strain *E. coli* MB43Δ*cydA* can be utilized for assessment of cytochrome *bd*-I functionality. This assay allows for rapid and convenient screening of mutants devoid of oxygen consumption activity, although it does not show strict quantitative correlation between growth rate and enzyme activity for mutants with intermediate activity. Nevertheless, this approach may also be applicable for the investigation of other components of the oxidative phosphorylation pathway, taking advantage of the ability of *E. coli* to grow in the absence of virtually the complete respiratory chain.

We found that deletion or shortening of the Q-loop insert did not yield functional cytochrome *bd*, despite using various approaches to shorten or exchange this domain. The low degree of plasticity of the Q-loop insert is surprising, as it can be expected that domains that are not ubiquitously found across species can be transferred without large impact on protein function. As an example, a region of ~35 residues involved in redox regulation is found in chloroplast ATP synthase, but not in homologous enzymes from bacterial or mammalian species [43]. It has been demonstrated that part of this region can be transferred to the F_1-ATPase from the cyanobacterium *Synechocystis* PCC 6803 [44] and the whole region can be transferred to the F_1-ATPase from the thermophilic *Bacillus* PS3 [45]. In both cases the transferred region imparted the susceptibility for redox regulation, without a significant impact on the target enzyme's stability and activity [44,45]. The requirement of the C-terminal Q-loop insert for basic cytochrome *bd*-I function and assembly/stability indicates a considerable degree of co-evolution between the Q-loop insert and other regions/subunits of cytochrome *bd*. In this regard, previous genetic analyses showed that the presence of the Q-loop insert correlated with the presence of the single-helix subunit CydX [34]. Genetic classification analyses indicated two basic types of cytochrome *bd*, distinguished by Q-loop length [1,46–48]. The evolutionary difference between the cytochrome *bd* enzymes carrying the C-terminal insert and those that lack this insert may be unexpectedly large.

Our results show that the C-terminal Q-loop insert is needed for

A

	cydABX (WT)	bd-II (240-389)	Insert bd-II	Gln^{313}-Arg^{317}	Leu^{328}-Arg^{332}	Lys^{348}-Gly^{352}	Gln^{373}- Lys^{377}
Purified protein (μg)	186 ± 14	152 ± 40	145 ± 83	159 ± 3	168 ± 25	136 ± 8	173± 14

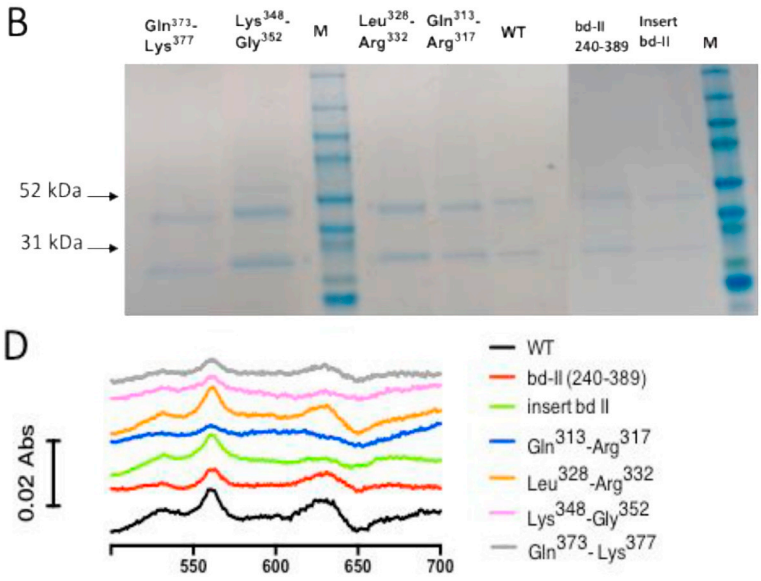

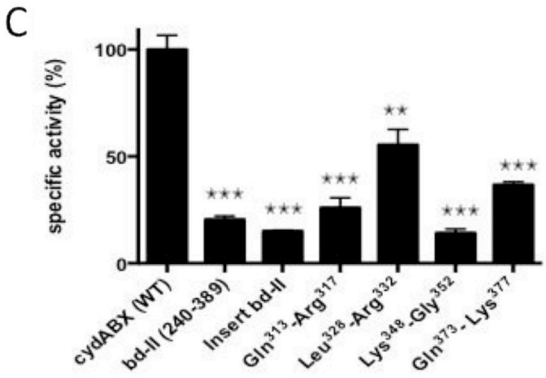

Fig. 7. Characterization of purified cytochrome *bd*-I Q-loop mutants. A: Yield of protein purified from 5 g wet bacteria. B: SDS-PAGE of purified cytochrome *bd*-I mutants. Lane M contains the Rainbow marker, 52 kDa and 31 kDa marker proteins are indicated. C: Oxygen consumption activity purified mutant protein as determined by Clark-type electrode using ubiquinone-1/DTT as substrate. The specific activity of the wild-type enzyme was ~100 μmol O_2/min/mg. Presented values are averages from two biological replicates (comprising in total six technical replicates), error bars represent SEM (★★★: $P < .001$, ★★: $P < .01$). D: Heme content of purified mutants. Reduced-minus-oxidized absorption spectra were recorded using 50 μg of purified protein. For more details, please refer to Material & methods.

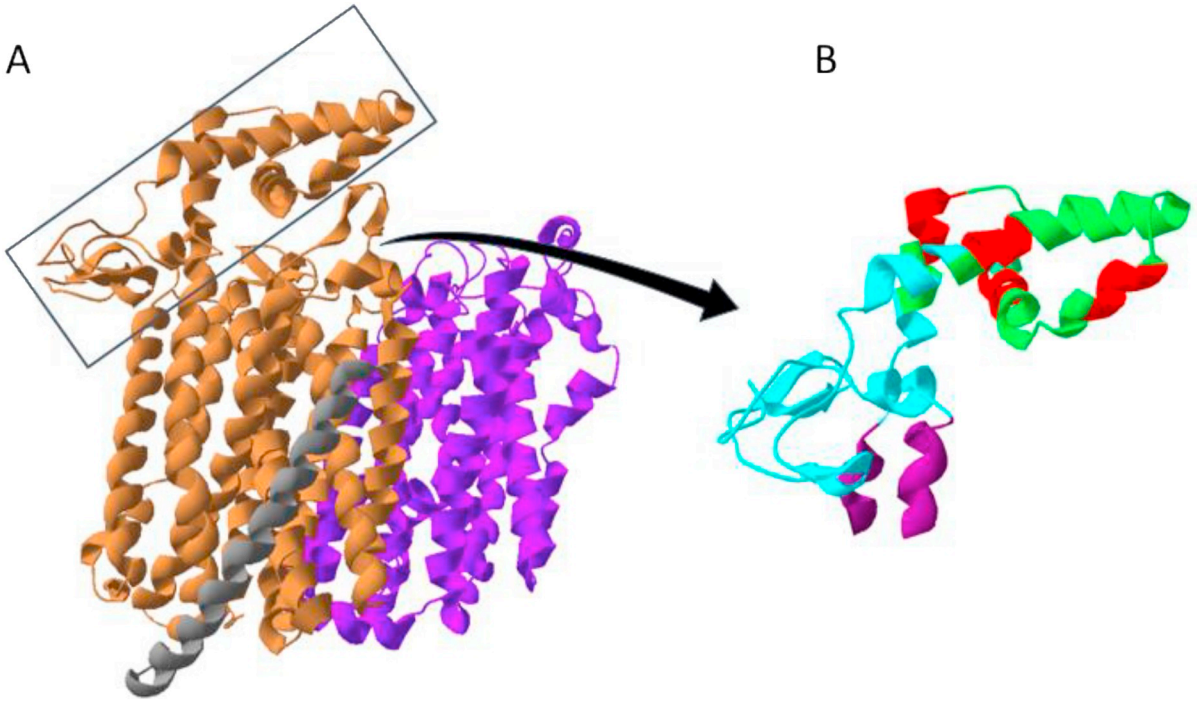

Fig. 8. Predicted structure of the Q-loop. A: Structure of CydABX cytochrome *bd*-I from *E. coli* as predicted (https://datadryad.org/resource/doi:10.5061/dryad.987j0) based on the Rosetta algorithm [49]. CydA is depicted in brown, CydB in purple and CydX in dark grey. B: The structure zoomed in on the Q-loop. Transmembrane helices 6 and 7 are shown in purple, the amino-terminal part of the Q-loop in light blue and the C-terminal insert in green. The four regions identified by alanine scanning mutagenesis are indicated in red.

proper binding of the heme cofactors and prevents stable assembly of the CydABX complex. Our data do not allow for pinpointing the molecular mechanism by which the Q-loop insert exerts this function. Based on the predicted interaction between the Q-loop insert and the CydX subunit [34] it can be speculated that deletion or mutation of the insert may lead to dissociation of CydX, which in turn may cause instability of the CydAB complex [26,27]. However, this predicted interaction has not been experimentally confirmed yet.

A de novo structure model based on the Rosetta algorithm for *E. coli* cytochrome *bd*-I predicted a largely helical conformation for the Q-loop insert (Fig. 8). The predicted location of the Q-loop insert is on top of CydA [49], where the insert may act as a rigid cover on the periplasmic side. Cryo-EM structures for *E. coli* cytochrome *bd*-I, which were published during the revision process of our manuscript, support this prediction [28,29]. As such, the Q-loop insert may prevent dissociation of bound heme groups and stabilize the whole CydABX complex. The four regions identified by alanine scanning mutagenesis in our study as essential for protein functionality according to this prediction are not clustered together, but located in various helices of the Q-loop insert (Fig. 7, red regions). It is unclear how these regions contribute to cytochrome *bd*-I assembly/stability. To answer this question, the newly published Cryo-EM structures *E. coli* cytochrome *bd*-I may facilitate site-directed mutagenesis experiments modifying individual residues within the insert, combined with mutagenesis of potential interaction partners elsewhere in CydABX.

Declaration of competing interest

The authors declare that they have no known competing financial interests or personal relationships that could have appeared to influence the work reported in this paper.

Acknowledgement

The authors are indebted to Jos Arends (University of Amsterdam) for generously providing the MB43 strain and to Anu Priyanka for assistance with figures.

Funding

This work was partly supported by a Grant-in-Aid for Scientific Research (C) (16K07299 to J.S.) from the Japan Society for the Promotion of Science and from the National Institutes of Health (HL16101 to R.B.G).

Author contributions

Hojjat Ghasemi Goojani: Conceptualization, Methodology, Investigation, Writing-Original Draft. Julia Konings: Investigation. Henk Hakvoort: Investigation. Sangjin Hong and Robert Gennis: Resources, Editing and Reviewing. Junshi Sakamoto: Conceptualization, Editing and Reviewing. Holger Lill: Resources, Editing and Reviewing. Dirk Bald: Conceptualization, Writing-Reviewing & Editing, Supervision.

Appendix A. Supplementary data

Supplementary data to this article can be found online at https://doi.org/10.1016/j.bbabio.2020.148175.

References

[1] V.B. Borisov, R.B. Gennis, J. Hemp, M.I. Verkhovsky, The cytochrome *bd* respiratory oxygen reductases, Biochim. Biophys. Acta 1807 (2011) 1398–1413.
[2] R. D'mello, S. Hill, R.K. Poole, The cytochrome *bd* quinol oxidase in *Escherichia coli* has an extremely high oxygen affinity and two oxygen-binding haems: implications for regulation of activity in vivo by oxygen inhibition, Microbiology 142 (1996) 755–763.
[3] B.D. Kana, E.A. Weinstein, D. Avarbock, S.S. Dawes, H. Rubin, V. Mizrahi, Characterization of the *cydAB*-encoded cytochrome *bd* oxidase from *Mycobacterium smegmatis*, J. Bacteriol. 183 (2001) 7076–7086.
[4] V.B. Borisov, E. Forte, P. Sarti, M. Brunori, A.A. Konstantinov, A. Giuffrè, Redox

control of fast ligand dissociation from *Escherichia coli* cytochrome *bd*, Biochem. Biophys. Res. Commun. 355 (2007) 97–102.
[5] M.G. Mason, M. Shepherd, P. Nicholls, P.S. Dobbin, K.S. Dodsworth, R.K. Poole, C.E. Cooper, Cytochrome *bd* confers nitric oxide resistance to *Escherichia coli*, Nat. Chem. Biol. 5 (2009) 94–96.
[6] A. Giuffrè, V.B. Borisov, M. Arese, P. Sarti, E. Forte, Cytochrome *bd* oxidase and bacterial tolerance to oxidative and nitrosative stress, Biochim. Biophys. Acta 1837 (2014) 1178–1187.
[7] M. Shepherd, M.E.S. Achard, A. Idris, M. Totsika, M.D. Phan, K.M. Peters, S. Sarkar, C.A. Ribeiro, L.V. Holyoake, D. Ladakis, G.C. Ulett, M.J. Sweet, R.K. Poole, A.G. McEvan, M.A. Schembri, The cytochrome *bd* I respiratory oxidase augments survival of multidrug-resistant *Escherichia coli* during infection, Sci. Rep. 6 (2016) 35285, https://doi.org/10.1038/srep35285.
[8] N.D. Hammer, M.L. Reniere, J.E. Cassat, Y. Zhang, A.O. Hirsch, M. Indriati Hood, E.P. Skaar, Two heme-dependent terminal oxidases power *Staphylococcus aureus* organ-specific colonization of the vertebrate host, MBio 4 (2013) e00241–13, https://doi.org/10.1128/mBio.00241-13.
[9] C.J. Beebout, A.R. Eberly, S.H. Werby, S.A. Reasoner, J.R. Brannon, S. De, M.J. Fitzgerald, M.M. Huggins, D.B. Clayton, L. Cegelski, M. Hadjifrangiskou, Respiratory heterogeneity shapes biofilm formation and host colonization in uropathogenic *Escherichia coli*, MBio 10 (2019) e02400–18, https://doi.org/10.1128/mBio.02400-18.
[10] A. Koul, L. Vranckx, N. Dhar, H.W.H. Göhlmann, E. Özdemir, J.M. Neefs, M. Schulz, L.P. Mortz E, J.D. McKinney, K. Andries, D. Bald, Delayed bactericidal response of *Mycobacterium tuberculosis* to bedaquiline involves remodelling of bacterial metabolism, Nat. Commun. 5 (2014) 3369, https://doi.org/10.1038/ncomms4369.
[11] K. Arora, B. Ochoa-Montaño, P.S. Tsang, T.L. Blundell, S.S. Dawes, V. Mizrahi, T. Bayliss, C.J. Mackenzie, L.A. Cleghorn, P.C. Ray, P.G. Wyatt, E. Uh, J. Lee, C.E. Barry 3rd, H.I. Boshoff, Respiratory flexibility in response to inhibition of cytochrome C oxidase in *Mycobacterium tuberculosis*, Antimicrob. Agents Chemother. 58 (2014) 6962–6965, https://doi.org/10.1128/AAC.03486-14.
[12] M. Berney, T.E. Hartman, W.R. Jacobs, A *Mycobacterium tuberculosis* cytochrome *bd* oxidase mutant is hypersensitive to bedaquiline, MBio 5 (4) (2014) e01275, https://doi.org/10.1128/mBio.01275-14.
[13] P. Lu, M.H. Heineke, A. Koul, K. Andries, G.M. Cook, H. Lill, R. van Spanning, D. Bald, The cytochrome *bd*-type quinol oxidase is important for survival of Mycobacterium smegmatis under peroxide and antibiotic-induced stress, Sci. Rep. 5 (2015) 10333, https://doi.org/10.1038/srep10333.
[14] K. Hards, J.R. Robson, M. Berney, L. Shaw, D. Bald, A. Koul, K. Andries, G.M. Cook, Bactericidal mode of action of bedaquiline, J. Antimicrob. Chemother. 70 (2015) 2028–2037.
[15] N.P. Kalia, E.J. Hasenoehrl, N.B. Ab Rahman, V.H. Koh, M.L.T. Ang, D.R. Sajorda, K. Hards, G. Grüber, S. Alonso, G.M. Cook, M. Berney, K. Pethe, Exploiting the synthetic lethality between terminal respiratory oxidases to kill *Mycobacterium tuberculosis* and clear host infection, Proc. Natl. Acad. Sci. USA 114 (2017), https://doi.org/10.1073/pnas.1706139114.
[16] L. Shi, C.D. Sohaskey, B.D. Kana, S. Dawes, R.J. North, V. Mizrahi, M.L. Gennaro, Changes in energy metabolism of Mycobacterium tuberculosis in mouse lung and under in vitro conditions affecting aerobic respiration, Proc. Natl. Acad. Sci. U. S. A. 102 (2005) 15629–15634, https://doi.org/10.1073/pnas.0507850102.
[17] M.J. Miller, R.B. Gennis, The purification and characterization of the cytochrome d terminal oxidase complex of the *Escherichia coli* aerobic respiratory chain, J. Biol. Chem. 258 (1983) 9159–9165.
[18] K. Kita, K. Konishi, Y. Anraku, Terminal oxidases of *Escherichia coli* aerobic respiratory chain. II. Purification and properties of cytochrome *b*558-*d* complex, J. Biol. Chem. 259 (1984) 3375–3381.
[20] S. Jünemann, J.M. Wrigglesworth, Cytochrome *bd* oxidase from *Azotobacter vinelandii*. Purification and quantitation of ligand binding to the oxygen reduction site, J. Biol. Chem. 270 (1995) 16213–16220.
[21] J. Sakamoto, A. Matsumoto, K. Oobuchi, N. Sone, Cytochrome *bd*-type quinol oxidase in a mutant of *Bacillus stearothermophilus* deficient in caa_3-type cytochrome *c* oxidase, FEMS Microbiol. Lett. 143 (1996) 151–158.
[22] S. Safarian, C. Rajendran, H. Müller, J. Preu, J.D. Langer, S. Ovchinnikov, T. Hirose, T. Kusumoto, J. Sakamoto, H. Michel, Structure of a *bd* oxidase indicates similar mechanisms for membrane-integrated oxygen reductases, Science 352 (2016) 583–586.
[23] K. Kusumoto, M. Sakiyama, J. Sakamoto, S. Noguchi, N. Sone, Menaquinol oxidase activity and primary structure of cytochrome *bd* from the amino-acid fermenting bacterium *Corynebacterium glutamicum*, Arch. Microbiol. 173 (2000) 390–397.
[24] M.G. Sturr, T.A. Krulwich, D.B. Hicks, Purification of a cytochrome *bd* terminal oxidase encoded by the *Escherichia coli* app locus from a delta cyo delta cyd strain complemented by genes from *Bacillus firmus* OF4, J. Bacteriol. 178 (1996) 1742–1749.
[25] V.B. Borisov, R. Murali, M.L. Verkhovskaya, D.A. Bloch, H. Han, R.B. Gennis, M.I. Verkhovsky, Aerobic respiratory chain of Escherichia coli is not allowed to work in fully uncoupled mode, Proc. Natl. Acad. Sci. U. S. A. 108 (2011) 17320–17324, https://doi.org/10.1073/pnas.1108217108.
[26] C.E. VanOrsdel, S. Bhatt, R.J. Allen, E.P. Brenner, J.J. Hobson, A. Jamil, B.M. Haynes, A.M. Genson, M.R. Hemm, The *Escherichia coli* CydX protein is a member of the CydAB cytochrome *bd* oxidase complex and is required for cytochrome bd oxidase activity, J. Bacteriol. 195 (2013) 3640–3650.
[27] J. Hoeser, S. Hong, G. Gehmann, R.B. Gennis, T. Friedrich, Subunit CydX of *Escherichia coli* cytochrome *bd* ubiquinol oxidase is essential for assembly and stability of the di-heme active site, FEBS Lett. 588 (2014) 1537–1541.
[28] S. Safarian, A. Hahn, D.J. Mills, M. Radloff, M.L. Eisinger, A. Nikolaev, J. Meier-Credo, F. Melin, H. Miyoshi, R.B. Gennis, J. Sakamoto, J.D. Langer, P. Hellwig, W. Kühlbrandt, H. Michel, Active site rearrangement and structural divergence in prokaryotic respiratory oxidases, Science. 366 (2019) 100–104.
[29] A. Theßeling, T. Rasmussen, S. Burschel, D. Wohlwend, J. Kägi, R. Müller, B. Böttcher, T. Friedrich, Homologous *bd* oxidases share the same architecture but differ in mechanism, Nat. Commun. 10 (2019) 5138, https://doi.org/10.1038/s41467-019-13122-4.
[30] A. Hata-Tanaka, K. Matsuura, S. Itoh, Y. Anraku, Electron flow and heme-heme interaction between cytochromes *b*-558, *b*-595 and *d* in a terminal oxidase of *Escherichia coli*, Biochim. Biophys. Acta 893 (1987) 289–295.
[31] J.P. Osborne, R.B. Gennis, Sequence analysis of cytochrome *bd* oxidase suggests a revised topology for subunits I, Biochim. Biophys. Acta 1410 (1999) 32–50.
[32] T.J. Dueweke, R.B. Gennis, Epitopes of monoclonal antibodies which inhibit ubiquinol oxidase activity of *Escherichia coli* cytochrome *d* complex localize a functional domain, J. Biol. Chem. 265 (1990) 4273–4277.
[33] T.J. Dueweke, R.B. Gennis, Proteolysis of the cytochrome *d* complex with trypsin and chymotrypsin localizes a quinol oxidase domain, Biochemistry 30 (1991) 3401–3406.
[34] R.J. Allen, E.P. Brenner, C.E. VanOrsdel, J.J. Hobson, D.J. Hearn, M.R. Hemm, Conservation analysis of the CydX protein yields insights into small protein identification and evolution, BMC Genomics 15 (2014) 946, https://doi.org/10.1186/1471-2164-15-946.
[35] R.M. Lorence, K. Carter, R.B. Gennis, K. Matsushita, H.R. Kaback, Trypsin proteolysis of the cytochrome *d* complex of Escherichia coli selectively inhibits ubiquinol oxidase activity while not affecting N,N,N′,N′-tetramethyl-p-phenylenediamine oxidase activity, J. Biol. Chem. 11 (1988) 5271–5276.
[36] R.G. Kranz, R.B. Gennis, Characterization of the cytochrome *d* terminal oxidase complex of *Escherichia coli* using polyclonal and monoclonal antibodies, J. Biol. Chem. 259 (1984) 7998–8003.
[37] T. Mogi, S. Akimoto, S. Endou, T. Watanabe-Nakayama, E. Mizuochi-Asai, H. Miyoshi, Probing the ubiquinol-binding site in cytochrome *bd* by site-directed mutagenesis, Biochem. Mosc. 45 (2006) 7924–7930.
[38] Y. Matsumoto, M. Murai, D. Fujita, K. Sakamoto, H. Miyoshi, M. Yoshida, T. Mogi, Mass spectrometric analysis of the ubiquinol-binding site in cytochrome *bd* from *Escherichia coli*, J. Biol. Chem. 281 (2006) 1905–1912.
[39] Y. Jiang, B. Chen, C. Duan, B. Sun, J. Yang, S. Yang, Multigene editing in the *Escherichia coli* genome via the CRISPR-Cas9 system, Appl. Environ. Microbiol. 81 (2015) 2506–2514.
[40] P. Lu, A.H. Asseri, M. Kremer, J. Maaskant, R. Ummels, H. Lill, D. Bald, The antimycobacterial activity of the cytochrome *bcc* inhibitor Q203 can be enhanced by small-molecule inhibition of cytochrome bd, Sci. Rep. 8 (2018) 2625, https://doi.org/10.1038/s41598-018-20989-8.
[41] H. Schägger, G. von Jagow, Tricine-sodium dodecyl sulfatepolyacrylamide gel electrophoresis for the separation of proteins in the range from 1 to 100 kDa, Anal. Biochem. 166 (1987) 368–379.
[42] M. Bekker, S. de Vries, A. Ter Beek, K.J. Hellingwerf, M.J. de Mattos, Respiration of *Escherichia coli* can be fully uncoupled via the nonelectrogenic terminal cytochrome *bd*-II oxidase, J. Bacteriol. 191 (2009) 5510–5517.
[43] T. Hisabori, H. Konno, H. Ichimura, H. Strotmann, D. Bald, Molecular devices of chloroplast F(1)-ATP synthase for the regulation, Biochim. Biophys. Acta 1555 (2002) 140–146.
[44] B.E. Krenn, P. Aardewijn, H.S. Van Walraven, S. Werner-Grüne, H. Strotmann, R. Kraayenhof, ATP synthase from a cyanobacterial *Synechocystis* 6803 mutant containing the regulatory segment of the chloroplast gamma subunit shows thiol modulation, Biochem. Soc. Trans. 23 (1995) 757–760.
[45] D. Bald, H. Noji, M.T. Stumpp, M. Yoshida, T. Hisabori, ATPase activity of a highly stable $\alpha_3\beta_3\gamma$ subcomplex of thermophilic F_1 can be regulated by the introduced regulatory region of γ subunit of chloroplast F_1, J. Biol. Chem. 275 (2000) 12757–12762.
[46] J. Sakamoto, N. Sone, Biochemical and molecular features of terminal oxidases, in: D. Zannoni (Ed.), Respiration in Archaea and Bacteria, Vol.1: Diversity of Prokaryotic Electron Transport Carriers, Series: Advances in Photosynthesis & Respiration, Vol. 15, Kluwer Academic Publishers, The Netherlands, 2004, pp. 87–113.
[47] A.M. Arutyunyan, J. Sakamoto, Y. Kabashima, Y. Inadome, V.B. Borisov, Optical and magneto-optical activity of cytochrome *bd* from *Geobacillus thermodenitrificans*, Biochim. Biophys. Acta 1817 (2012) 2087–2094.
[48] M. Degli Esposti, T. Rosas-Pérez, L.E. Servín-Garcidueñas, L.M. Bolaños, M. Rosenblueth, E. Martínez-Romero, Molecular evolution of cytochrome *bd* oxidases across proteobacterial genomes, Genome Biol Evol. 7 (2015) 801–820, https://doi.org/10.1093/gbe/evv032.
[49] S. Ovchinnikov, L. Kinch, H. Park, Y. Liao, J. Pei, D.E. Kim, H. Kamisetty, N.V. Grishin, D. Baker, Large-scale determination of previously unsolved protein structures using evolutionary information, Elife 4 (2015) e09248, https://doi.org/10.7554/eLife.09248.